

# We are IntechOpen, the world's leading publisher of Open Access books Built by scientists, for scientists

4,800

Open access books available

122,000

International authors and editors

135M

Downloads

Our authors are among the

154

Countries delivered to

TOP 1%

most cited scientists

12.2%

Contributors from top 500 universities



WEB OF SCIENCE™

Selection of our books indexed in the Book Citation Index  
in Web of Science™ Core Collection (BKCI)

Interested in publishing with us?  
Contact [book.department@intechopen.com](mailto:book.department@intechopen.com)

Numbers displayed above are based on latest data collected.  
For more information visit [www.intechopen.com](http://www.intechopen.com)



# Solar Thermochemical Fuel Generation

*Hongsheng Wang*

## Abstract

Solar energy is one of the most abundant, clean, and widespread energy in the world, which has the potential to address the issues of environmental pollution, global warming, and energy crisis, while the intermittent distribution of solar energy in time and space limits its utilization. Among various approaches of solar energy utilization, converting solar energy into chemical fuel (e.g., hydrogen) by thermochemical approach could maintain the steady and high-efficient energy supply and can make use of the full-spectrum solar energy. The research about solar thermochemical fuel generation lasts more than 40 years, and lots of reaction system and reactors have been proposed. This chapter reviews the state-of-the-art progress of solar thermochemical fuel generation, and the characteristics of different systems have been compared and discussed, which may give systematical insight into the development and improvement of solar fuel generation by thermochemical approach in the future.

**Keywords:** solar energy, solar fuel, solar thermochemistry, thermochemical fuel, solar membrane reactor

## 1. Introduction

### 1.1 Energy and environmental problems and solutions

Due to population growth and rapid industrial development, world energy demand has increased significantly. Compared with the previous generation, the world's population has increased rapidly by 2 billion [1], and this mainly comes from the population growth of developing countries, and rapid population growth poses more severe challenges to increasingly scarce energy and resource supplies. The importance of energy for social development is self-evident. In order to ensure the supply of energy, a large amount of fossil energy is used, which at the same time has a serious impact on the environment, leading to increasingly serious problems of atmospheric pollution and the greenhouse effect. Therefore, improving energy efficiency and using more clean energy and exploring a sustainable development path compatible with energy use and the environment have become one of the important topics in energy science research.

The efficient use of renewable energy is of great significance. Among the many renewable energy sources, solar energy has become one of the best choices for future energy sources with its unique advantages, which is the most abundant renewable energy source and widely distributed.

## 1.2 Advantages of solar thermochemical fuel generation

Solar energy is a huge amount of clean energy. It is of great significance to develop and utilize solar energy reasonably and efficiently. However, the efficient use of solar energy also faces limitations, such as the low energy density of solar energy, the unstable energy supply, the discontinuous time and spatial distribution of solar radiation, and the difficulty of direct storage [2, 3]. Therefore, solar energy is converted into chemical energy stored in fuels, which is generally considered to be an effective solution to make up for solar defects [2–6].

There are mainly four approaches for converting solar energy into chemical energy to generate solar fuel, which is illustrated in **Figure 1**. The photobiological process is limited by the low energy conversion efficiency now, and it is still at a very early stage of the development [7]. The other three methods have their own properties and have attracted lots of attention. Photo-electrolysis approach is most convenient, but it is also limited by the conversion rate, and researchers are seeking for the catalysts which have better performance. The electrolysis using photovoltaic (PV) materials and electrolyzer is the most mature approach for producing solar fuel. However, the PV materials can only utilize the light with a certain range of wavelength (usually short wavelength light), and the other part of sunlight absorbed is converted into thermal energy, which is wasted as residual heat, leading to a limited PV cell efficiency (the commercial PV cell efficiency is about 15%; the highest multiple-junction PV cell efficiency in lab is higher than 40% with high cost). The total energy efficiency from solar energy to chemical energy is the product of solar power efficiency (e.g., PV cell efficiency) and electrolysis efficiency, so the total efficiency has potential to be further improved. Compared with electrolysis, solar fuel generation by thermochemistry can utilize the sunlight with whole solar spectrum, which has a high theoretical energy efficiency. So the solar thermochemical fuel generation is a promising method and will be discussed in this chapter in details.

**Figure 2** is a schematic diagram of the solar thermochemical energy conversion process. Solar energy with lower energy density is received by solar collectors and converted into solar thermal energy. Solar thermal energy enters the absorber through heat transfer and drives the chemical reaction, so that low-energy-density solar energy is stored in the form of solar fuel as chemical energy with high energy density, which is relatively easy for storage and transportation. The sustainable and stable use of solar energy is achieved by transporting solar fuel to remote and needed places for power generation and chemical processes, etc., and solving the

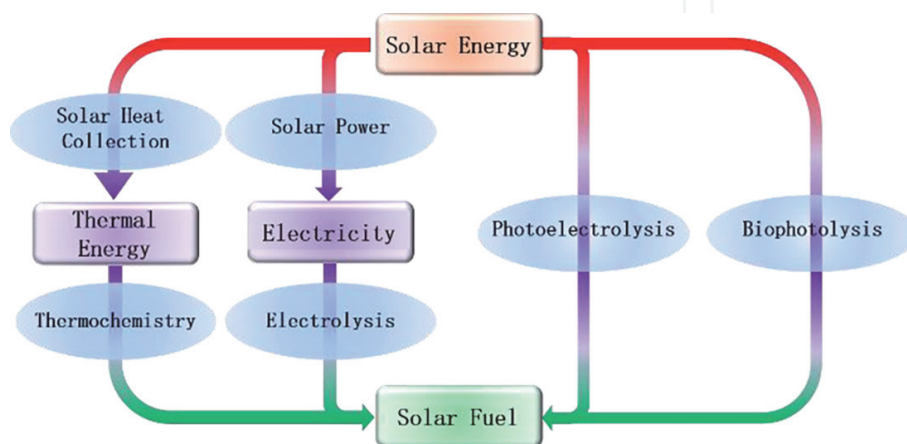


**Figure 1.**  
Illustration of solar fuel via various approaches.

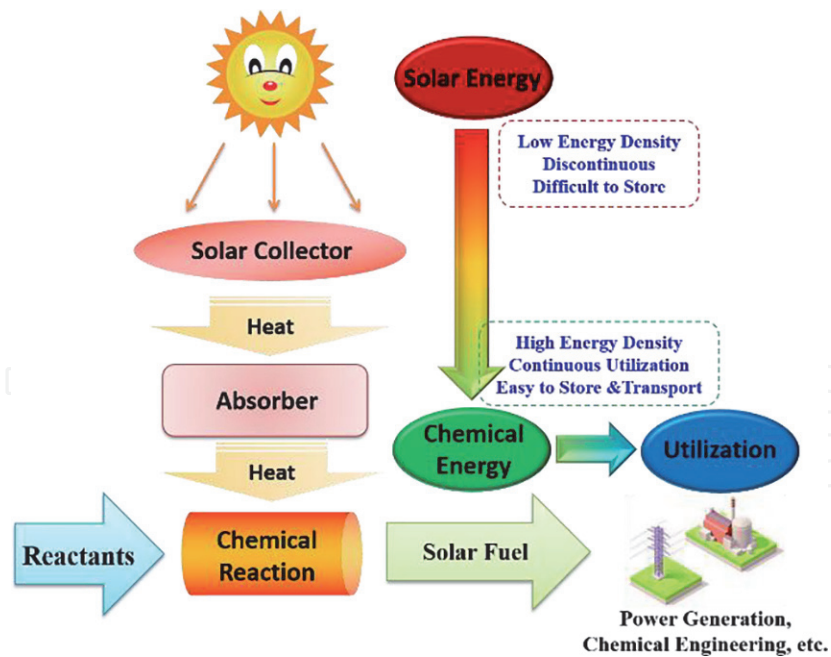


**Figure 2.**  
 Illustration of solar thermochemical energy conversion process.

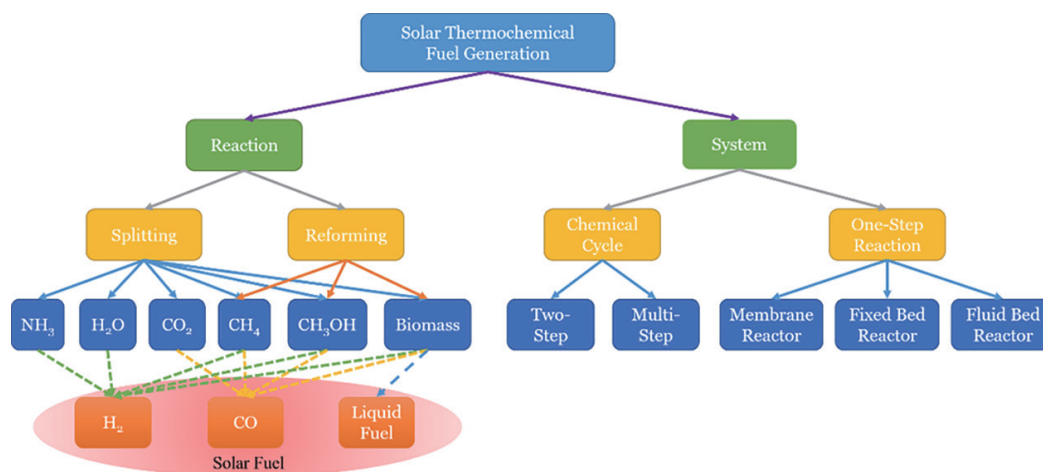


**Figure 3.**  
 Classification of solar thermochemical fuel generation.

discontinuity of solar distributed in time and space by means of chemical energy storage.

There are many researches about the reaction and system for solar thermochemical fuel generation published, and some of the significant parts have been classified in **Figure 3**. The two main fuels from solar energy are hydrogen and carbon monoxide, which both have great higher heating values and are potential to be utilized in the future, especially hydrogen, as hydrogen has the following characteristics:

1. Rich hydrogen energy reserves. On the earth, hydrogen mainly exists in the form of hydrocarbons and water, and more than 70% of the earth's surface is covered by water. Therefore, the earth contains a huge amount of hydrogen and has great potential for development.
2. The energy density of hydrogen is large. The higher heating value of hydrogen is much higher than that of hydrocarbons and alcohol compounds, and the consumption of hydrogen energy is increasing every year.

3. Hydrogen is renewable. Hydrogen can be obtained from water, and the oxidation of hydrogen produces water. Therefore, the hydrogen combustion and energy release cycle does not consume other substances.
4. Hydrogen energy is clean energy. Whether hydrogen is consumed by direct combustion or fuel cell power generation, the only product is water, without any waste pollution, which is clean and environmentally friendly.
5. Hydrogen is relatively easy to be converted and stored. Compared with other energy sources such as solar energy, wind energy, electrical energy, and thermal energy, hydrogen is a chemical raw material and is easily to be converted into hydrocarbons for storage, thereby expanding the scope of hydrogen energy in time and space.

### 1.3 Thermodynamic of solar thermochemical process

Different chemical reaction processes require different temperatures, so it is necessary to match the solar thermal energy temperature with the chemical reaction temperature for efficient energy utilization. Different solar thermal temperatures need to be achieved with different forms of solar collectors for matching various chemical reactions.

The heat collection temperature of solar collectors depends on many factors, but the most important factor is the concentration ratio, which is the ratio of the total area of the opening of the collector mirror field to the spot area on the focal plane. Concentration ratio is an important parameter for designing concentrating solar thermal utilization. Under the same conditions, the higher the concentration ratio, the higher the heat collection temperature. In a unit of time, the energy emitted by a black body per unit area is proportional to the fourth power of its temperature, and solar energy is close to a 6000 K black body, so the radiant energy it emits is:

$$Q_s = 4\pi r^2 \sigma T_s^4 \quad (1)$$

Among them,  $T_s$  is the absolute surface temperature of the sun and  $\sigma$  is the Stefan-Boltzmann constant. If the orbit of the earth is regarded as a circle with a radius  $R$ , as shown in **Figure 4**, the energy that  $Q_s$  throws on the absorber of area  $A$  is:

$$Q_{S \rightarrow A} = A \cdot \frac{Q_s}{4\pi R^2} \quad (2)$$

After the absorber absorbs energy, the temperature will rise. Assuming the temperature rises to  $T_a$ , if the conduction and convection losses are ignored, the absorber will radiate energy, given as:

$$Q_a = a\sigma T_a^4 \quad (3)$$

According to the second law of thermodynamics, heat can only be transferred spontaneously from a high-temperature object to a low-temperature object, so the temperature  $T_a$  of the absorber is always less than or equal to the solar surface temperature. In the limit, the two temperatures are equal, that is,  $T_a = T_s$ , and the amount of heat absorbed by the device is equal to the amount of radiation:

$$Q_{S \rightarrow A} - Q_a = A \cdot \frac{Q_s}{4\pi R^2} - a\sigma T_a^4 = 0 \quad (4)$$



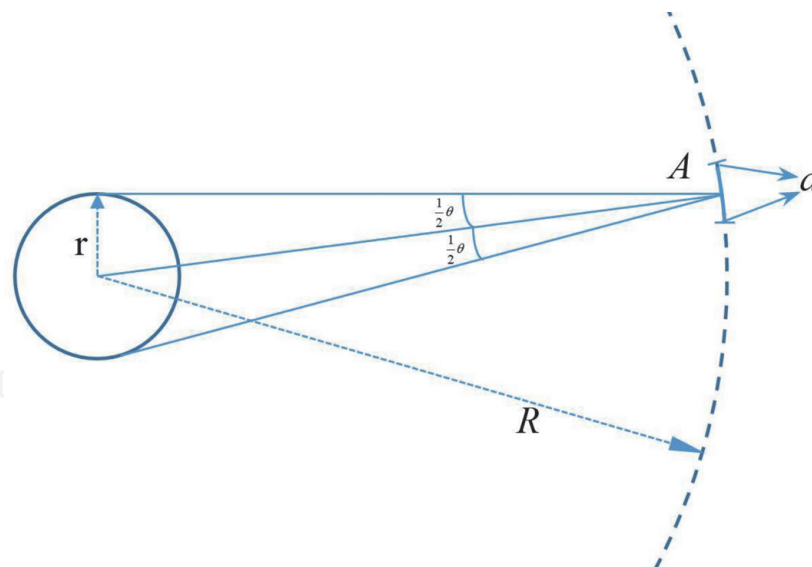


**Figure 4.**  
 Illustration of solar radiation trajectory.

According to the definition of the concentration ratio, it is:

$$C = \frac{A}{a} = \frac{R^2}{r^2} = \frac{1}{\sin^2 \frac{\theta}{2}} \quad (5)$$

Among them,  $\theta$  is the opening angle of the sun, and the value is  $32'$ , so the theoretical limiting concentration ratio is 45,000. In practical applications, the light ratio is much lower than the theoretical condenser ratio, due to manufacturing errors (misfocus, specular errors, etc.), structural disturbances, unsatisfactory optical properties (specular reflectance, glass absorptivity, etc.), shadows and sun tracking, etc.

In the actual application process, there are two types of common solar concentrating forms: linear focusing and point focusing. Among them, linear focusing solar collectors include parabolic trough solar collectors and linear Fresnel solar collectors. Because the collectors have different heat collection methods, they also have different light collection ratios and heat collection temperatures. Because point-focused solar collector focuses in two dimensions and line-focused solar collector focuses in one-dimensional directions, point-focused solar collectors usually have a larger concentration ratio, which could approach a greater temperature. However, high temperature usually means higher requirements for materials and processing industries, higher radiation losses, and heat costs of the collector. **Table 1** lists the typical solar thermal power generation mirror field parameters. In thermal power plants, a higher temperature for power generation will allow the Rankine cycle to have a higher Carnot efficiency, leading to a greater power generation efficiency.

In the process of collecting solar energy by using a solar collector, energy is dissipated due to radiation. The absorption efficiency is defined as the ratio of the solar energy absorbed by the absorption cavity to the total solar energy projected by the collector into the absorption cavity, given as [18]:

$$\eta_{abs} = \frac{IA\eta_A\alpha - a\epsilon\sigma T^4}{IA} \quad (6)$$

$\eta_{abs}$  is the absorption efficiency;  $I$  is the solar radiation intensity;  $A$  is the area of the condenser;  $\eta_A$  is the optical efficiency;  $\alpha$  and  $\epsilon$  are the absorptance and emissivity of the absorption cavity;  $a$  is the area of the absorber;  $\sigma$  is the Stefan-Boltzmann

Type	Annual power generation efficiency (%)	Peak efficiency (%)	Operating temperature (°C)	Concentration ratio
Parabolic trough collector power plant	14	25	400	30–100
Linear Fresnel collector power plant	13	18	300–400	30
Disc collector power plant	20	32	550–750	1000–10,000
Tower collector power plant	16	22	400–600	500–5000

**Table 1.** Performance parameters of typical solar collector fields [8–17].

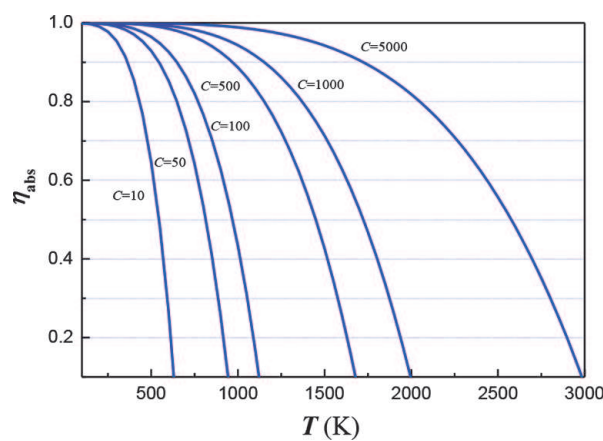


**Figure 5.** The relationship among the ideal absorption efficiency of the collector, the concentration ratio, and the heat collection temperature.

constant ( $5.67 \times 10^{-8} \text{W}/(\text{m}^2 \times \text{K}^4)$ ); and  $T$  is the set thermal temperature. If it is assumed that the absorption cavity is black body, then  $\eta_A$ ,  $\alpha$ , and  $\varepsilon$  are all 1, the above formula can be simplified as:

$$\eta_{abs} = 1 - \frac{\sigma T^4}{IC} \quad (7)$$

where  $C$  is the concentration ratio. If  $I = 1000 \text{W}/\text{m}^2$ , the relationship curve between the ideal absorption efficiency of the collector, the concentration ratio, and heat collection temperature can be obtained through calculation, as shown in **Figure 5**. When the heat collection temperature is fixed, the heat collection efficiency increases with the increase of the concentration ratio; when the concentration ratio is determined, the heat collection efficiency is a decreasing function of the heat collection temperature, mainly because as the heat collection temperature increases, the temperature difference between reactor and environment rises up, leading to an increase in radiation loss, which reduces the efficiency of heat collection.

With multiplying the obtained absorption efficiency by the Carnot cycle efficiency, the system efficiency can be obtained, which is the maximum theoretical conversion efficiency from the solar thermal energy obtained to work or electricity [18]:

$$\eta_s = \left( \frac{T_H - T_0}{T_H} \right) \left( 1 - \frac{\sigma T_H^4}{IC} \right) \quad (8)$$

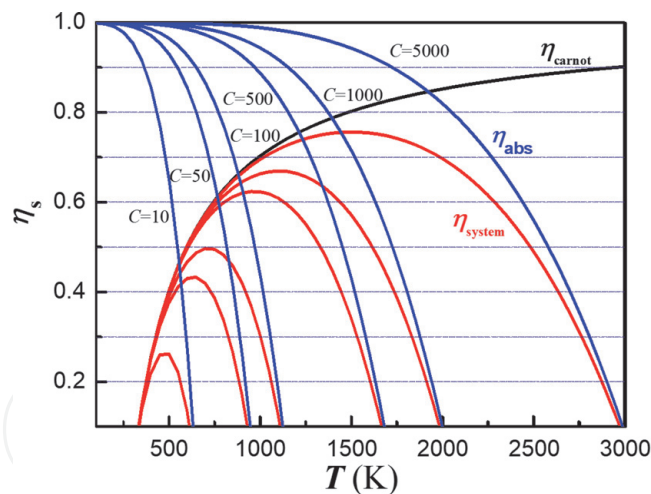


**Figure 6.**  
 The relationship among the maximum efficiency from solar thermal energy to work, the concentration ratio, and the heat collection temperature.

where  $T_H$  is the heat collection temperature of the solar collector and  $T_0$  is the ambient temperature. The calculation results are shown in **Figure 6**.

When decomposing water to produce hydrogen without relying on fossil energy, the temperature required for thermochemical reactions is about 1300–1800°C. According to **Figures 5 and 6**, it can be seen that a tower or dish collector with a concentration ratio of 5000 should be selected. When using fossil fuel (e.g., methane) to split water for hydrogen generation, the reaction temperature could be decreased to 700–1000°C. A tower or dish solar concentrator with a concentration ratio of 1000 should be used. The reaction temperature of the novel solar hydrogen permeation membrane alternating cycle methane reforming system introduced later in this chapter is about 350–400°C, and a trough solar concentrator with a concentration ratio of 80–100 is enough for it, which has a much lower cost compared with tower or the dish-type solar concentrating collector.

According to Eq. (8), when the concentration ratio  $C$  is given, the first-order derivative function of can be obtained, shown as Eq. (9):

$$\frac{d\eta_s}{dT} = \frac{T_0}{T_H^2} + \frac{\sigma T_H^2(3T_0 - 4T_H)}{IC} \quad (9)$$

By maintaining Eq. (9) equal to 0, the optimal heat collection temperature can be obtained at a given concentration ratio, and the optimal heat collection

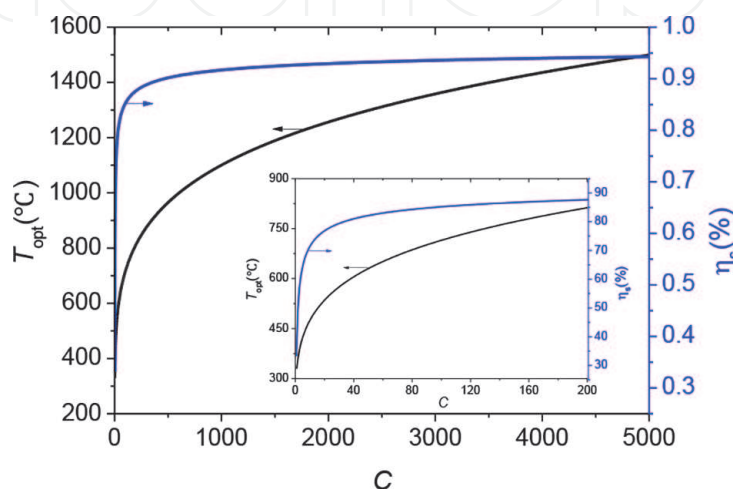


**Figure 7.**  
 Variation of maximum theoretical efficiency from solar energy to work and optimal thermal energy collection temperature with concentration ratio.



temperature can be substituted into Eq. (8) to obtain the sun at the best heat collection temperature. The maximum theoretical efficiency from solar energy to work is shown in **Figure 7**.

From **Figure 7**, as the concentration ratio increases, the intensity of radiation received per unit area of the collector increases, so both the optimal heat collection temperature and the maximum theoretical efficiency increase. Because the solar collector has a fixed concentration ratio in practical applications, **Figure 7** has guiding significance for determining the optimal heat-collecting temperature for a solar heat collector with a specific concentration ratio. The solar thermal energy of the system has the maximum work efficiency at the best concentration ratio.

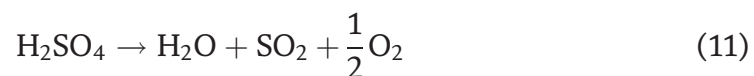
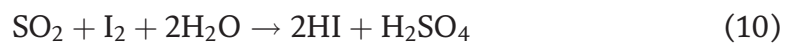
## 2. Thermochemical cycle

The existing thermochemical cycle for hydrogen production mainly includes metal oxide system thermochemical cycle, sulfur-containing system, sulfuric acid decomposition method, metal-halide system, and reformed methane hydrogen production. All of the thermochemical cycles could be classified as multi-step thermochemical cycles and two-step thermochemical cycles.

### 2.1 Multi-step thermochemical cycles

#### 2.1.1 Hydrogen generation system containing sulfur

There are four main types of hydrogen production in sulfur-containing systems: iodine-sulfur cycle,  $\text{H}_2\text{SO}_4\text{-H}_2\text{S}$  cycle, sulfuric acid-methanol cycle, and sulfate cycle. Among them, the iodine-sulfur cycle is the most famous. It was invented by the United States GA company in the 1970s, so it is also called the GA cycle. The process is shown in **Figure 8**. The main reaction process is as follows:



GA company found [19] that the excess  $\text{I}_2$  exists, and HI and  $\text{H}_2\text{SO}_4$  can be separated into two liquid phases, which is the basis for the development of the IS cycle. The advantages of the IS cycle are using of thermal energy below  $1000^\circ\text{C}$  for hydrogen generation, closed circuit, only water being needed to be added in the circulation process, and the expected efficiency which can reach 52%. The disadvantages are concentrated sulfuric acid being highly corrosive when heated at high temperature; the equilibrium decomposition ratio of HI being low (20%); and the reaction intermediate products sulfur dioxide and iodine being easy to cause pollution and liable to have side reactions.

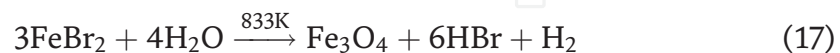
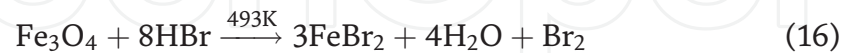
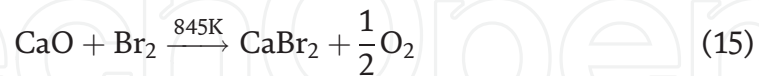
#### 2.1.2 Sulfuric acid decomposition method

This type of method is best known as the Westinghouse cycle [20], and its main process is shown in **Figure 9**. The highest temperature in the process needs to be above  $800^\circ\text{C}$ , and the efficiency of the cycle can reach 40%. If multi-stage electrolysis is used, it can reach 46%. However, the disadvantage is that concentrated

sulfuric acid is highly corrosive at high temperatures and has high requirements for material selection.

### 2.1.3 Metal-halide system

The most famous in this system is the UT-3 cycle proposed by the University of Tokyo. The main process is as follows:



Sakurai [21] found that the hydrolysis of calcium bromide was the slowest during this cycle, because the calcium oxide agglomerated, reducing the reaction interface area. The addition of lauric acid as a foaming agent for dispersing the calcium oxide aggregates can improve the performance of the reaction. The Argonne National Laboratory in the United States has also researched and developed this process [22]. Its main feature is the decomposition or formation of

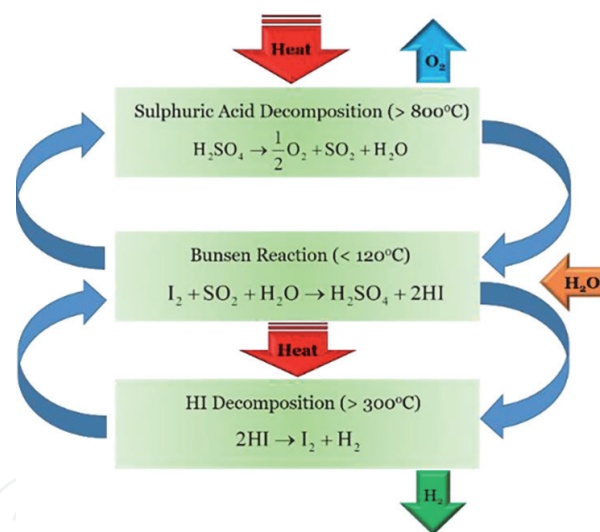


**Figure 8.**  
 Illustration of iodine-sulfur cycle.

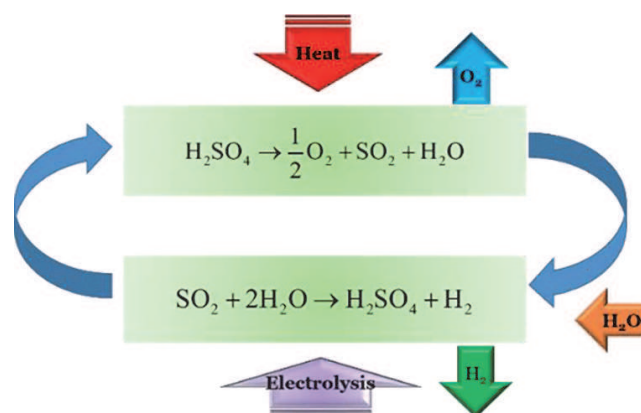


**Figure 9.**  
 Westinghouse cycle diagram.

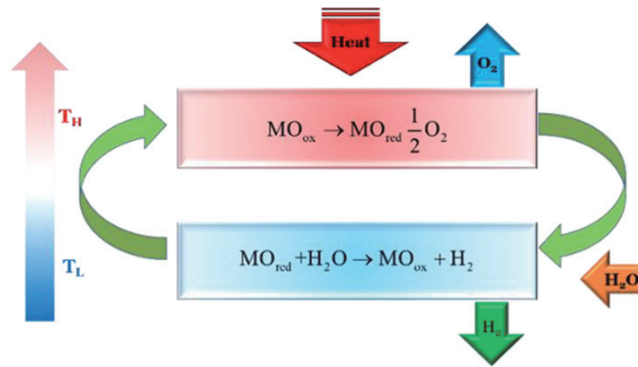


**Figure 10.**  
Metal oxide thermochemical cycle for hydrogen production.

HBr by electrolytic method or “cold” plasma method. This reaction has the following advantages: its expected thermal efficiency is 35–40%, and if the power is generated at the same time, the overall efficiency can be improved by 10%; the two-step key reaction is a gas-solid reaction, which significantly simplifies the separation of products and reactants; the elements used are cheap and readily available; the process involves only solid and gaseous reactants and products. However, the separation of intermediate products in the reaction process is also a problem and challenge in the process.

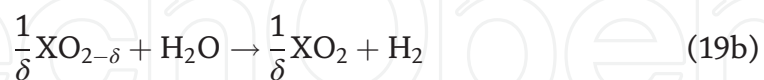
## 2.2 Two-step thermochemical cycles

The common two-step thermochemical cycle hydrogen production process is mainly metal oxide thermochemical cycle, which has the following three forms:

Oxide:



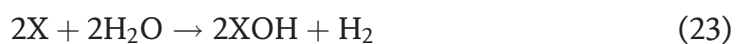
or



Hydride:



Hydroxide:



Among them, metal oxide thermochemical hydrogen production is the most common. The process is shown in **Figure 10**.

As shown in **Figure 10**, metal oxides are reduced by releasing oxygen at high temperatures, and oxidized with water at low temperatures, taking away oxygen

atoms from water molecules to generate hydrogen. During the thermochemical cycle, metal oxides can be reduced to simple metals, such as:

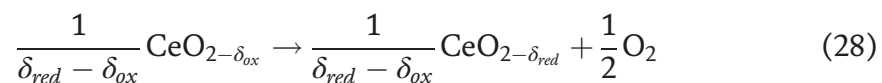


Metal oxides may also be reduced from higher valence to lower valence oxides, such as:

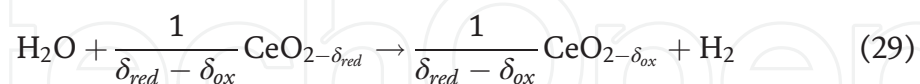


Among them, metal Zn is easy to form a dense oxide film, which is wrapped on the metal surface to prevent the reaction from proceeding. Wegner et al. [23] designed a spray reactor for solving this problem. By increasing the specific surface area of metal Zn to increase the contact area in the reaction, the experiment proves that the chemical conversion of Zn can reach 83%. The disadvantage of this method is that the metal Zn needs to be gasified and atomized, which requires large energy consumption; Zn, Sn, and other metals are also easily oxidized again during the decomposition process, affecting the reaction efficiency. The oxidation rate of iron oxide is easily reduced due to sintering, and ferrite has strong reducing ability. It can reduce CO<sub>2</sub> to C solid element and cover the surface of ferrite to prevent the reaction from proceeding. One of the materials currently considered to be the most suitable for the thermochemical cycle of metal oxides is cerium oxide (CeO<sub>2</sub>), because cerium oxide can efficiently reduce water or carbon dioxide to hydrogen or carbon monoxide [24], and cerium oxide also has good anti-coking properties. The specific reaction equations are:

High temperature (reduction step):



Low temperature (oxidation step):

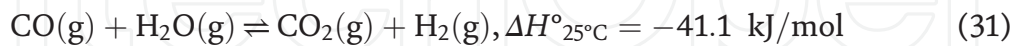
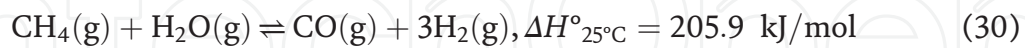


In the two-step thermochemical cycle hydrogen production process, because there is a large heat transfer temperature difference between the “oxidation step” and “reduction step” (e.g., the temperature difference between cerium oxide heat transfer is about 700°C), the thermal energy recovery of solid materials has always been a very difficult problem. Hao et al. [25] proposed an “isothermal” thermochemical cycle, that is, the “oxidation step” and “reduction step” reactions are performed at the same temperature. The “isothermal” thermochemical cycle effectively overcomes the defect that a large amount of solid sensible heat in the “dual-temperature” thermochemical cycle cannot be efficiently recovered and does not generate thermal stress, which can maintain high energy utilization efficiency at high temperatures. However, the isothermal thermochemical cycle also has certain limitations that need to be resolved, such as the requirement of maintaining a quite low oxygen partial pressure, less hydrogen production in a single cycle, etc. The thermochemical cycle with metal oxide can also be utilized for CO generation from CO<sub>2</sub>, and the thermodynamics is similar to that of H<sub>2</sub> generation from H<sub>2</sub>O, which will not be discussed here.

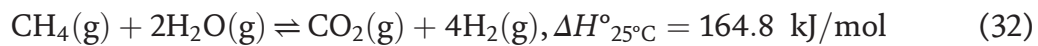
### 3. Carbon feed-based solar thermochemistry

#### 3.1 Methane reforming and decomposition

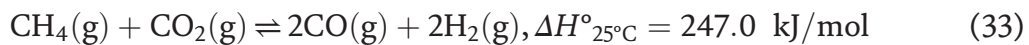
Nowadays, more than 95% of the hydrogen for refinery use is produced via hydrocarbon steam reforming [26]. Industrial hydrogen production through methane steam reforming exceeds 50 million tons annually and accounts for 2–5% of global energy consumption [27]. Methane steam reforming process for hydrogen production is usually described by the following reactions:



where the reversible water-gas shift reaction Eq. (11) is sometimes considered as superimposed onto the methane reforming reaction Eq. (10) for conveniences of analysis on methane conversion:



The methane dry reforming is the reaction between methane and carbon dioxide for syngas generation, given as:



The reforming reactions, Eqs. (10), (12), and (13), are highly endothermic, and a large amount of heat is often provided by burning a supplemental amount of methane [28], which will decrease the heat value of fuel gas generated by 22% for the same amount of methane consumed and release large amounts of greenhouse gas  $\text{CO}_2$  [29]. In recent years, as the technologies of concentrated solar energy (CSE) and solar thermal utilization improve rapidly, methane reforming driven by CSE emerged as a promising method for hydrogen production [30], which derives heat from solar energy instead of fossil fuels. Besides, solar thermal energy with relatively low temperatures (compared with methane combustion) is absorbed by methane reforming reaction and upgraded to the chemical energy with higher energy level (ratio of exergy change  $\Delta E$  to enthalpy change  $\Delta H$  of a process [31]) in such process. Solar energy thus stored in hydrogen as chemical energy, and it could be converted into power with significantly greater efficiencies than that of solar-thermal-only power generation in the same temperature range [32].

In order to achieve the high-efficient progress of the solar methane reforming reaction, research on solar methane reforming reactors has also continued. Klein et al. [33] proposed a schematic diagram of a fluidized bed reactor. This experiment is a methane dry reforming experiment, where gas reactants and carbon particles are mixed and passed into the reactor together. The reactor can achieve a concentration ratio of 3000 through primary and secondary light concentration, and the reaction temperature is between 950 and 1450°C with the ratio of carbon dioxide to methane changes from 1: 1 to 6: 1, which has a maximum methane conversion of 90%. Edwards et al. [34] studied methane steam reforming in a solar tubular reactor, which is condensed by a 107 m<sup>2</sup> dish condenser. The condensing temperature can reach 850°C, and the pressure can reach 20 bars. The reactor can stably produce hydrogen, but there is no detailed introduction on the conversion rate in the literature. The device for hydrogen production by metal oxide thermochemical cycling was proposed by Steinfeld et al. [35]. The system contains a 51.8 m<sup>2</sup> heliostat to focus the sunlight at first, and then the sunlight passed through a parabolic surface with an opening area of 2.7 m<sup>2</sup> to focus it again. The final focusing ratio was



Participant	$Q_{\text{solar}}$ (kW)	Pressure (bar)	$T$ (K)	Reactor type	Reactant conversion (%)	Efficiency (%)	Ref.
PSI	5	>1	1600	Vortex flow	64	15.1 <sup>a</sup> , 16.2 <sup>b</sup>	[37]
PSI	5	>1	1600	Particle flow	99	16.1 <sup>b</sup>	[38]
PROMES- CNRS	10	0.4	1773	Tubular	98	4.8 <sup>b</sup>	[39, 40]
PROMES- CNRS	50	0.45	1928	Tubular	100	13.5 <sup>a</sup> , 15.2 <sup>b</sup>	[41]
NREL	6	1	2133	Aerosol flow	90	2 <sup>b</sup>	[42]
PROMES- CNRS	0.8	0.61	1700	Nozzle type	95	5.9 <sup>a</sup>	[43]

<sup>a</sup> $\eta_{\text{chemical}} = \frac{\Delta H_{\text{react}}^{\circ} T_{\text{reactor}}}{Q_{\text{solar}}}$  – accounts for the energy required to drive the reaction.

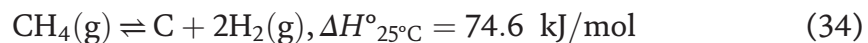
<sup>b</sup> $\eta_{\text{thermal}} = X_{\text{reaction}} \cdot \dot{m}_{\text{CH}_4} \cdot \frac{\Delta H_{\text{react}}^{\circ} T_{\text{reactor}}}{Q_{\text{solar}}}$  – accounts for the energy required to heat the reactants and effect the reaction.

**Table 2.**

Summary of experimental research on solar methane decomposition [36].

3500. During the reaction, ZnO particles with an average particle diameter of 0.4  $\mu\text{m}$  were sent into a cylindrical reaction chamber for reaction by methane. The products were Zn simple substance and synthesis gas ( $\text{H}_2$ , CO). The reactor can reach 50% methane conversion at 1030°C.

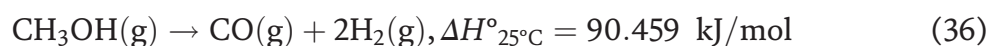
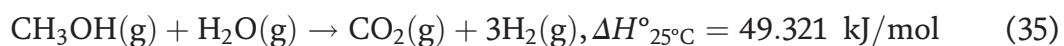
Methane decomposition is also an endothermic reaction at 600–1200°C, given as:



Solar methane decomposition has been researched in both indirectly and directly heated reactors from solar thermal energy. A summary of experimental study has been listed in **Table 2**.

### 3.2 Methanol reforming and decomposition

Methanol reforming and decomposition also attracts lots of attention in the field of solar thermochemical fuel generation [44], as the reaction temperature is about 150–300°C, which is quite low and easy to be maintained by line-focusing solar collector (parabolic trough collector or linear Fresnel lens) with low cost. The reaction equations of methanol reforming and decomposition are given as:



Both of the two reactions are endothermic, which can convert the low-level solar thermal energy (low temperature) into high-level chemical energy, and have been researched with combining with other systems, like PV cell module, and combined cooling heating and power in downstream.

### 3.3 Biomass gasification

Biomass is widespread and is often perceived as a carbon-neutral source of energy. Solar biomass gasification is a clean route to obtain fuels, which may also reach liquid fuel for vehicle or jet utilization. Detailed reviews on solar biomass

Feed	$Q_{\text{solar}}$ (kW)	$T$ (K)	Gasifying agent	Reactor type	Reactant conversion (%)	Product yield (%)	Efficiency (%)	Ref.
Bituminous coal	1.2	1600	CO <sub>2</sub>	Fluidized bed quartz tubular reactor	65	—	8 <sup>a</sup>	[49]
Pet coke	5	1818	Steam	Vortex flow	87	35 (H <sub>2</sub> ), 15 (CO)	9 <sup>a</sup> , 20 <sup>b</sup>	[50]
Pet coke— water slurry	5	1500	Steam	Vortex flow	87	65 (H <sub>2</sub> ), 25 (CO)	4.7 <sup>a</sup> , 17.4 <sup>b</sup>	[51]
Petroleum VR	5	1573	Steam	Vortex flow	50	68 (H <sub>2</sub> ), 15 (CO)	2 <sup>c</sup> , 19 <sup>a</sup>	[52]
Coal coke	0.94	1123	CO <sub>2</sub>	Internally circulating fluidized bed	—	—	12 <sup>a</sup>	[53]
IS, SS, STP, fluff, SAC, beech charcoal	5	1490	Steam	Packed bed	100	H <sub>2</sub> / CO = 1.5, CO <sub>2</sub> / CO = 0.2	29 <sup>d</sup> , $U = 1.3^e$	[54]
Beech charcoal	3	1523	Steam	Particle flow reactor	30	—	1.53 <sup>b</sup>	[55]
Coal coke	1.1	1573	CO <sub>2</sub>	Fluidized bed	42	—	14 <sup>a</sup>	[56]
Coal coke	3	1773	CO <sub>2</sub>	Internally circulating fluidized bed	73	—	12 <sup>f</sup>	[57]
LRK, tire chips, Fluff, DSS, IS, SB	150	1350– 1453	Steam	Packed bed	36–100	H <sub>2</sub> / CO = 2– 5.2	25–35 <sup>d</sup> , $U = 1.03–$ 1.30 <sup>e</sup>	[58]

$$^a \eta_{\text{chemical}} = \frac{\dot{Q}_{\text{chem}}}{Q_{\text{solar}}}$$

$$^b \eta_{\text{thermal}} = \frac{\dot{Q}_{\text{chem}} + \dot{Q}_{\text{sensible}}}{Q_{\text{solar}} + Q_{\text{steam}}}$$

$$^c \eta_{\text{process}} = \frac{\dot{n}_{\text{H}_2} LHV_{\text{H}_2} + \dot{n}_{\text{CO}} LHV_{\text{CO}} + \sum_i^{\text{species}} \int_{473\text{K}}^{T_{\text{reactor}}} \dot{n}_i C_{p,i}(T) dT}{Q_{\text{solar}} + Q_{\text{steam}} + \dot{n}_{\text{VR}} LHV_{\text{VR}}}$$

$$^d \eta_{\text{solar-to-chemical}} = \frac{m_{\text{syngas}} LHV_{\text{syngas}}}{m_{\text{fs}} LHV_{\text{fs}} + Q_{\text{solar}}}$$

$$^e U = \frac{m_{\text{syngas}} LHV_{\text{syngas}}}{m_{\text{fs}} LHV_{\text{fs}}}$$

$$^f \eta_{\text{energy}} = \frac{\Delta H_{298\text{K}} R_{\text{CO}}}{Q_{\text{input}} + \frac{Q_{\text{gas}}}{\eta_{\text{receiver}}}}$$

**Table 3.** Summary of experimental research published in gasification of solid hydrocarbon feed [36].

gasification have been conducted by Epstein et al. [45], Lédé [46], Nzihou et al. [47], and Puig-Arnavat et al. [48], which will not be discussed here. A summary of experimental work published in gasification of solid hydrocarbon feed has been listed in **Table 3**.

#### 4. Solar thermochemical fuel generation by membrane reactor

Solar thermochemistry usually requires high temperature (e.g., above 4000°C for H<sub>2</sub>O splitting; 3000°C for CO<sub>2</sub> splitting; 700–1000°C for methane reforming),

which requires high concentration ratio and large mirror area, and the system will be more complex and expensive. In situ separation by a permeable membrane for a target product shifts thermodynamic equilibrium of chemical reactions in favor of reactants conversion, which equivalently lowers solar collection temperature. Combination of membrane reactor and solar thermal collection offers unique advantages in many respects, such as the increment of conversion rate, decrease of reaction temperature, and emission reduction, which are otherwise unattainable by either alone. Besides, the all-solid-state feature and isothermal operation enable compact design of solar fuel reactors with minimized thermal stress. Now, the selective permeation membrane for gas species in high temperature is mainly oxygen permeation membrane, hydrogen permeation membrane, and carbon dioxide permeation membrane, which have been researched for solar thermochemical fuel generation.

#### **4.1 Oxygen permeation membrane for H<sub>2</sub>O/CO<sub>2</sub> splitting**

Perovskites, ZrO<sub>2</sub> and CeO<sub>2</sub> (or doped ZrO<sub>2</sub> and CeO<sub>2</sub>), usually constitute the selective oxygen permeation membrane utilized in high temperature (>600°C). Wang et al. [59] proposed a theoretical framework for the thermodynamic analysis of solar oxygen permeation membrane reactor, and the solar-to-fuel efficiency (ratio of the higher heating value of products to the total energy input) can reach as high as 89% in methane-assisted membrane reactor. Zhu et al. [60] brought up a thermodynamic model of ceria dense membrane for CO<sub>2</sub> splitting, and the energy efficiency is above 10% at 1800 K without heat recovery. Steinfeld et al. [61, 62] have done a lot of experimental researches about solar CO<sub>2</sub> splitting for CO generation by oxygen permeation membrane with 100% selectivity (e.g., La<sub>0.6</sub>Sr<sub>0.4</sub>Co<sub>0.2</sub>Fe<sub>0.8</sub>O<sub>3-δ</sub> at 1030°C [61], CeO<sub>2</sub> at 1600°C [62]), and Ozin [63] said the research of Steinfeld is an elegant demonstration and an exciting breakthrough for continuous CO<sub>2</sub> splitting in a single step, at a single temperature, in a single reactor.

#### **4.2 Hydrogen permeation membrane for hydrogen generation**

The materials of the hydrogen permeation membrane are various, such as metal (e.g., palladium, nickel), perovskites, pyrochlores, fluorites, polymers, which are usually used in the reaction of reforming, splitting, partial oxidation of hydrocarbon, splitting of other hydrogen carriers (e.g., NH<sub>3</sub>), and water-gas shift reaction. Li et al. [30] first presented an innovative solar-assisted hybrid power system integrated with methane steam reforming in membrane reactor, and the simulation results showed that capture ratio of CO<sub>2</sub> is 91% and exergy efficiency and thermal efficiency are 58 and 51.6% (10.2 and 2.2% points higher than the CO<sub>2</sub> capture from exhaust cycle), respectively. Said et al. [64] simulated a CFD model about solar molten salt-heated H<sub>2</sub>-selective membrane reformer for methane upgrading and hydrogen generation, and the results showed the fuel heating value upgrade of 40% with methane conversion rate of 99% and hydrogen recovery of 87% at 600°C. Wang et al. [65] put forward a novel reactor, which realized direct methane steam reforming in parabolic trough collector integrated with hydrogen permeation membrane reactor, and the system can perform high and stable efficiency (above 80%) at 400°C. Mallapragada et al. [66] proposed a novel system that consists of oxygen permeation membrane and hydrogen permeation membrane for solar water splitting, and the solar-to-H<sub>2</sub> efficiency (ratio of the lower heating value of hydrogen to the reversible work input for Gibbs free energy change of water splitting) is 72.4–80.1% at the concentration ratios of 2000–10,000. Sui et al. [67] reported an exploration on an efficient solar thermochemical water-splitting system enhanced

by hydrogen permeation membrane, which has showed a sharply enhanced conversion rate of 87.8% at 1500°C and  $10^{-5}$  bar at permeated side (versus 1.26% with oxygen permeation membrane or isothermal thermochemical cycle). Recently, a promising method for hydrogen generation without carbon emitting by ammonia decomposition in a catalytic palladium membrane reactor for hydrogen separation driven by solar energy has been theoretically proposed, and the first-law thermodynamic efficiency, net solar-to-hydrogen efficiency, and exergy efficiency can reach as high as 86.86, 40.08, and 72.07%, respectively [68].

### 4.3 Carbon dioxide permeation membrane for hydrocarbon reforming

Carbon dioxide permeation membrane includes mixed  $e^-/CO_3^{2-}$  conducting membrane,  $O^{2-}/CO_3^{2-}$  conducting membrane,  $OH^-/CO_3^{2-}$  conducting membrane (hydroxide/ceramic dual-phase membrane), etc. [69, 70]. The combination between carbon dioxide permeation membrane and solar energy is very limited now. The combination of hydrogen permeation membrane and carbon dioxide permeation membrane has been proposed for methane steam reforming by way of an alternate  $H_2$  and  $CO_2$  separation driven by solar energy [71]. The carbon dioxide permeation membrane has great potential to be utilized for the hydrocarbon reforming or decomposition for  $CO_2$  separation and capture in the future.

### 4.4 Challenges and perspectives

Though the solar membrane reactor has lots of advantages and immense potential for application mentioned above, the efficient approach to lower the partial pressure of gas product (or avoid the relatively low pressure) is the main challenge to maintain a high energy conversion rate, and the improvement of stability and permeability of membrane material at corresponding reaction temperature is also significant. These issues have potential areas for big breakthroughs and require further studies to address. The multiple product separation with membrane reactor may be a promising method to increase the energy efficiency, due to a relatively high partial pressure and less separation energy required [71].

## 5. Conclusions

This chapter has reviewed the state-of-the-art researches about solar thermochemical fuel generation, and the highlighted conclusions are listed:

- a. The thermodynamics in solar thermochemical fuel generation has been analyzed, and the maximum theoretical efficiency from solar energy to work has been obtained.
- b. The most representative solar thermochemical reactions (e.g.,  $H_2O/CO_2$  splitting, hydrocarbon reforming, and decomposition) have been reviewed, and the advantages and drawbacks have been analyzed and discussed.
- c. Thermochemical cycle and membrane reactor driven by solar energy have been systematically introduced, which could decrease the reaction temperature and have the potential to be widely utilized in the future, especially the membrane reactor, which could purify the product with a continuous operation.

## **Acknowledgements**

This work is funded by the National Natural Science Foundation of China (no. 51906179) and the State Scholarship Fund (No. 201906275035) from China Scholarship Council.

IntechOpen

## **Author details**

Hongsheng Wang<sup>1,2</sup>

1 Wuhan University, Wuhan, China

2 The University of Tokyo, Tokyo, Japan

\*Address all correspondence to: [wanghongsheng@whu.edu.cn](mailto:wanghongsheng@whu.edu.cn)

## **IntechOpen**

---

© 2020 The Author(s). Licensee IntechOpen. This chapter is distributed under the terms of the Creative Commons Attribution License (<http://creativecommons.org/licenses/by/3.0>), which permits unrestricted use, distribution, and reproduction in any medium, provided the original work is properly cited. 



## References

- [1] Kannan N, Vakeesan D. Solar energy for future world: a review. *Renewable and Sustainable Energy Reviews*. 2016; **62**:1092-1105. DOI: 10.1016/j.rser.2016.05.022
- [2] Simakov DSA, Wright MM, Ahmed S, Mokheimer EMA, Román-Leshkov Y. Solar thermal catalytic reforming of natural gas: A review on chemistry, catalysis and system design. *Catalysis Science & Technology*. 2015; **5**: 1991-2016. DOI: 10.1039/C4CY01333F
- [3] Kong H, Hao Y, Wang H. A solar thermochemical fuel production system integrated with fossil fuel heat recuperation. *Applied Thermal Engineering*. 2016; **108**:958-966. DOI: 10.1016/j.applthermaleng.2016.03.170
- [4] Kong H, Kong X, Wang H, Wang J. A strategy for optimizing efficiencies of solar thermochemical fuel production based on nonstoichiometric oxides. *International Journal of Hydrogen Energy*. 2019; **44**(36):19585-19594. DOI: 10.1016/j.ijhydene.2019.05.197
- [5] Fletcher EA. On the thermodynamics of solar energy use. *Journal of the Minnesota Academy of Science*. 1983; **49**:30-34
- [6] Wang H, Li W, Liu T, Liu X, Hu X. Thermodynamic analysis and optimization of photovoltaic/thermal hybrid hydrogen generation system based on complementary combination of photovoltaic cells and proton exchange membrane electrolyzer. *Energy Conversion and Management*. 2019; **183**:97-108. DOI: 10.1016/j.enconman.2018.12.106
- [7] Yilanci A, Dincer I, Ozturk HK. A review on solar-hydrogen/fuel cell hybrid energy systems for stationary applications. *Progress in Energy and Combustion Science*. 2009; **35**(3):231-244. DOI: 10.1016/j.pecs.2008.07.004
- [8] Lovegrove K, Wes S. *Concentrating solar power technology: Principles, developments and applications*. Cambridge, UK: Elsevier; 2012
- [9] IRENA. *Renewable Energy Cost Analysis—Concentrating Solar Power*. Abu Dhabi, United Arab Emirates: International Renewable Energy Agency; 2012
- [10] IRENA. *Renewable Power Generation Costs in 2014*. Abu Dhabi, United Arab Emirates: International Renewable Energy Agency; 2014
- [11] SunShot. *SunShot Vision Study*. Golden, USA: U.S. Department of Energy; 2012
- [12] Ayre J. New solar stirling dish efficiency record of 32% set. *Clean Technica*. 2013; **17**. Available from: <https://cleantechnica.com/2013/01/17/new-solar-stirling-dish-efficiency-record-of-32-set/>
- [13] Siva Reddy V, Kaushik SC, Ranjan KR, Tyagi SK. State-of-the-art of solar thermal power plants—A review. *Renewable and Sustainable Energy Reviews*. 2013; **27**:258-273. DOI: 10.1016/j.rser.2013.06.037
- [14] Pavlović TM, Radonjić IS, Milosavljević DD, Pantić LS. A review of concentrating solar power plants in the world and their potential use in Serbia. *Renewable and Sustainable Energy Reviews*. 2012; **16**(6):3891-3902. DOI: 10.1016/j.rser.2012.03.042
- [15] Kaygusuz K. Prospect of concentrating solar power in Turkey: The sustainable future. *Renewable and Sustainable Energy Reviews*. 2011; **15**(1): 808-814. DOI: 10.1016/j.rser.2010.09.042
- [16] Weinstein LA, Loomis J, Bhatia B, Bierman DM, Wang EN, Chen G. *Concentrating solar power*. Chemical

Reviews. 2015;**115**(23):12797-12838.  
DOI: 10.1021/acs.chemrev.5b00397

[17] Steinfeld A, Palumbo R. Solar thermochemical process technology. *Encyclopedia of Physical Science and Technology*. 2001;**15**(1):237-256

[18] Fletcher EA, Moen RL. Hydrogen and oxygen from water. *Science*. 1977;**197**(4308):1050-1056. DOI: 10.1126/science.197.4308.1050

[19] Zhang P, Yu B, Chen J, Xu J. Study on the hydrogen production by thermochemical water splitting. *Progress in Chemistry*. 2005;**17**(4): 643-650

[20] Spewock S, Brecher LE, Talko F. The thermal catalytic decomposition of sulfur trioxide to sulfur dioxide and oxygen. In: *Proceedings of the 1st World Hydrogen Energy Conference*. Coral Gables, FL: University of Miami Press. p. 1976

[21] Sakurai M, Bilgen E, Tsutsumi A, Yoshida K. Adiabatic UT-3 thermochemical process for hydrogen production. *International Journal of Hydrogen Energy*. 1996;**21**(10):865-870. DOI: 10.1016/0360-3199(96)00024-9

[22] Doctor RD, Dacid CW, Mendelsohn MH. *AICHE Spring National Meeting*; New Orleans, 2002.

[23] Wegner K, Ly HC, Weiss RJ, Pratsinis SE, Steinfeld A. In situ formation and hydrolysis of Zn nanoparticles for H<sub>2</sub> production by the 2-step ZnO/Zn water-splitting thermochemical cycle. *International Journal of Hydrogen Energy*. 2006;**31**(1):55-61. DOI: 10.1016/j.ijhydene.2005.03.006

[24] Chueh WC, Falter C, Abbott M, Scipio D, Furler P, Haile SM, et al. High-flux solar-driven thermochemical dissociation of CO<sub>2</sub> and H<sub>2</sub>O using nonstoichiometric ceria. *Science*. 2010;

**330**:1797-1801. DOI: 10.1126/science.1197834

[25] Hao Y, Yang CK, Haile SM. High-temperature isothermal chemical cycling for solar-driven fuel production. *Physical Chemistry Chemical Physics*. 2013;**15**(40):17084-17092

[26] Collodi G, Wheeler F. Hydrogen production via steam reforming with CO<sub>2</sub> capture. *Chemical Engineering Transactions*. 2010;**19**:37-42

[27] Saavedra J, Whittaker T, Chen Z, Pursell CJ, Rioux RM, Chandler BD. Controlling activity and selectivity using water in the Au-catalysed preferential oxidation of CO in H<sub>2</sub>. *Nature Chemistry*. 2016;**8**:584-589. DOI: 10.1038/nchem.2494

[28] Barelli L, Bidini G, Gallorini F, Servili S. Hydrogen production through sorption-enhanced steam methane reforming and membrane technology: A review. *Energy*. 2008;**33**(4):554-570. DOI: 10.1016/j.energy.2007.10.018

[29] Fan J, Zhu L. Performance analysis of a feasible technology for power and high-purity hydrogen production driven by methane fuel. *Applied Thermal Engineering*. 2015;**75**:103-114. DOI: 10.1016/j.applthermaleng.2014.10.013

[30] Li Y, Zhang N, Cai R. Low CO<sub>2</sub>-emissions hybrid solar combined-cycle power system with methane membrane reforming. *Energy*. 2013;**58**:36-44. DOI: 10.1016/j.energy.2013.02.005

[31] Ishida M, Kawamura K. Energy and exergy analysis of a chemical process system with distributed parameters based on the enthalpy-direction factor diagram. *Industrial & Engineering Chemistry Process Design and Development*. 1982;**21**(4):690-695

[32] Han W, Jin H, Zhang N, Zhang X. Cascade utilization of chemical energy of natural gas in an improved CRGT

- cycle. *Energy*. 2007;**32**(4):306-313. DOI: 10.1016/j.energy.2006.06.014
- [33] Klein HH, Karni J, Rubin R. Dry methane reforming without a metal catalyst in a directly irradiated solar particle reactor. *Journal of Solar Energy Engineering*. 2009;**131**(2):021001-1-021001-14. DOI: 10.1115/1.3090823
- [34] Edwards JH, Duffy GJ, Benito R, Do T, Dave N, McNaughton R, et al. CSIRO's solar thermal-fossil energy hybrid technology for advanced power generation. In: *Proceedings of Solar Thermal 2000 10th SolarPACES International Symposium on Solar Thermal Concentrating Technologies*; Sydney, N.S.W. 2000. pp. 27-32
- [35] Steinfeld A, Brack M, Meier A, Weidenkaff A, Wuillemin D. A solar chemical reactor for co-production of zinc and synthesis gas. *Energy*. 1998; **23**(10):803-814. DOI: 10.1016/S0360-5442(98)00026-7
- [36] Yadav D, Banerjee R. A review of solar thermochemical processes. *Renewable and Sustainable Energy Reviews*. 2016;**54**:497-532. DOI: 10.1016/j.rser.2015.10.026
- [37] Hirsch D, Steinfeld A. Solar hydrogen production by thermal decomposition of natural gas using a vortex-flow reactor. *International Journal of Hydrogen Energy*. 2004; **29**(1):47-55. DOI: 10.1016/S0360-3199(03)00048-X
- [38] Maag G, Zanganeh G, Steinfeld A. Solar thermal cracking of methane in a particle-flow reactor for the co-production of hydrogen and carbon. *International Journal of Hydrogen Energy*. 2009;**34**(18):7676-7685. DOI: 10.1016/j.ijhydene.2009.07.037
- [39] Rodat S, Abanades S, Sans JL, Flamant G. Hydrogen production from solar thermal dissociation of natural gas: Development of a 10 kW solar chemical reactor prototype. *Solar Energy*. 2009; **83**(9):1599-1610. DOI: 10.1016/j.solener.2009.05.010
- [40] Maag G, Rodat S, Flamant G, Steinfeld A. Heat transfer model and scale-up of an entrained-flow solar reactor for the thermal decomposition of methane. *International Journal of Hydrogen Energy*. 2010;**35**(24):13232-13241. DOI: 10.1016/j.ijhydene.2010.08.119
- [41] Rodat S, Abanades S, Sans JL, Flamant G. A pilot-scale solar reactor for the production of hydrogen and carbon black from methane splitting. *International Journal of Hydrogen Energy*. 2010;**35**(15):7748-7758. DOI: 10.1016/j.ijhydene.2010.05.057
- [42] Dahl JK, Buechler KJ, Weimer AW, Lewandowski A, Bingham C. Solar-thermal dissociation of methane in a fluid-wall aerosol flow reactor. *International Journal of Hydrogen Energy*. 2004;**29**(7):725-736. DOI: 10.1016/j.ijhydene.2003.08.009
- [43] Abanades S, Flamant G. Production of hydrogen by thermal methane splitting in a nozzle-type laboratory-scale solar reactor. *International Journal of Hydrogen Energy*. 2005;**30**(8):843-853. DOI: 10.1016/j.ijhydene.2004.09.006
- [44] Liu Q, Hong H, Yuan J, Jin H, Cai R. Experimental investigation of hydrogen production integrated methanol steam reforming with middle-temperature solar thermal energy. *Applied Energy*. 2009;**86**(2):155-162. DOI: 10.1016/j.apenergy.2008.03.006
- [45] Epstein M, Spiewak I, Funken KH, Ortner J. Review of the technology for solar gasification of carbonaceous materials. *Solar Engineering*. 1994; **26**(13):79-91
- [46] Lédé J. Solar thermochemical conversion of biomass. *Solar Energy*.



1999;65(1):3-13. DOI: 10.1016/S0038-092X(98)00109-1

[47] Nzihou A, Flamant G, Stanmore B. Synthetic fuels from biomass using concentrated solar energy—A review. *Energy*. 2012;42(1):121-131. DOI: 10.1016/j.energy.2012.03.077

[48] Puig-Arnavat M, Tora EA, Bruno JC, Coronas A. State of the art on reactor designs for solar gasification of carbonaceous feedstock. *Solar Energy*. 2013;97:67-84. DOI: 10.1016/j.solener.2013.08.001

[49] Kodama T, Kondoh Y, Tamagawa T, Funatoh A, Shimizu KI, Kitayama Y. Fluidized bed coal gasification with CO<sub>2</sub> under direct irradiation with concentrated visible light. *Energy & Fuels*. 2002;16(5):1264-1270. DOI: 10.1021/ef020053x

[50] Z'Graggen A, Haueter P, Trommer D, Romero M, De Jesus JC, Steinfeld A. Hydrogen production by steam-gasification of petroleum coke using concentrated solar power—II. Reactor design, testing, and modeling. *International Journal of Hydrogen Energy*. 2006;31(6):797-811. DOI: 10.1016/j.ijhydene.2005.06.011

[51] Z'Graggen A, Haueter P, Maag G, Vidal A, Romero M, Steinfeld A. Hydrogen production by steam-gasification of petroleum coke using concentrated solar power—III. Reactor experimentation with slurry feeding. *International Journal of Hydrogen Energy*. 2007;32(8):992-996. DOI: 10.1016/j.ijhydene.2006.10.001

[52] Z'Graggen A, Steinfeld A. Hydrogen production by steam-gasification of carbonaceous materials using concentrated solar energy—V. Reactor modeling, optimization, and scale-up. *International Journal of Hydrogen Energy*. 2008;33(20):5484-5492. DOI: 10.1016/j.ijhydene.2007.10.038

[53] Kodama T, Enomoto SI, Hatamachi T, Gokon N. Application of an internally circulating fluidized bed for windowed solar chemical reactor with direct irradiation of reacting particles. *Journal of Solar Energy Engineering*. 2008;130(1):014504. DOI: 10.1115/1.2807213

[54] Piatkowski N, Wieckert C, Steinfeld A. Experimental investigation of a packed-bed solar reactor for the steam-gasification of carbonaceous feedstocks. *Fuel Processing Technology*. 2009;90(3):360-366. DOI: 10.1016/j.fuproc.2008.10.007

[55] Melchior T, Perkins C, Lichty P, Weimer AW, Steinfeld A. Solar-driven biochar gasification in a particle-flow reactor. *Chemical Engineering and Processing: Process Intensification*. 2009;48(8):1279-1287. DOI: 10.1016/j.cep.2009.05.006

[56] Kodama T, Gokon N, Enomoto SI, Itoh S, Hatamachi T. Coal coke gasification in a windowed solar chemical reactor for beam-down optics. *Journal of Solar Energy Engineering*. 2010;132(4):041004. DOI: 10.1115/1.4002081

[57] Gokon N, Ono R, Hatamachi T, Liuyun L, Kim HJ, Kodama T. CO<sub>2</sub> gasification of coal cokes using internally circulating fluidized bed reactor by concentrated Xe-light irradiation for solar gasification. *International Journal of Hydrogen Energy*. 2012;37(17):12128-12137. DOI: 10.1016/j.ijhydene.2012.05.133

[58] Wieckert C, Obrist A, Zedtwitz PV, Maag G, Steinfeld A. Syngas production by thermochemical gasification of carbonaceous waste materials in a 150 kWth packed-bed solar reactor. *Energy & Fuels*. 2013;27(8):4770-4776. DOI: 10.1021/ef4008399

[59] Wang H, Hao Y, Kong H. Thermodynamic study on solar

thermochemical fuel production with oxygen permeation membrane reactors. *International Journal of Energy Research*. 2015;**39**(13):1790-1799. DOI: 10.1002/er.3335

[60] Zhu L, Lu Y, Shen S. Solar fuel production at high temperatures using ceria as a dense membrane. *Energy*. 2016;**104**:53-63. DOI: 10.1016/j.energy.2016.03.108

[61] Michalsky R, Neuhaus D, Steinfeld A. Carbon dioxide reforming of methane using an isothermal redox membrane reactor. *Energy Technology*. 2015;**3**(7):784-789. DOI: 10.1002/ente.201500065

[62] Tou M, Michalsky R, Steinfeld A. Solar-driven thermochemical splitting of CO<sub>2</sub> and in situ separation of CO and O<sub>2</sub> across a ceria redox membrane reactor. *Joule*. 2017;**1**(1):146-154. DOI: 10.1016/j.joule.2017.07.015

[63] Ozin GA. "One-pot" solar fuels. *Joule*. 2017;**1**(1):19-23. DOI: 10.1016/j.joule.2017.08.010

[64] Said SA, Simakov DS, Waseeuddin M, Román-Leshkov Y. Solar molten salt heated membrane reformer for natural gas upgrading and hydrogen generation: A CFD model. *Solar Energy*. 2016;**124**:163-176. DOI: 10.1016/j.solener.2015.11.038

[65] Wang H, Liu M, Kong H, Hao Y. Thermodynamic analysis on mid/low temperature solar methane steam reforming with hydrogen permeation membrane reactors. *Applied Thermal Engineering*. 2019;**152**:925-936. DOI: 10.1016/j.applthermaleng.2018.03.030

[66] Mallapragada DS, Agrawal R. Limiting and achievable efficiencies for solar thermal hydrogen production. *International Journal of Hydrogen Energy*. 2014;**39**(1):62-75. DOI: 10.1016/j.ijhydene.2013.10.075

[67] Sui C, Wang H, Liu X, Hu X. Solar thermochemical water-splitting reaction enhanced by hydrogen permeation membrane. arXiv preprint arXiv: 1808.02175. 2018

[68] Wang B, Kong H, Wang H, Wang Y, Hu X. Kinetic and thermodynamic analyses of mid/low-temperature ammonia decomposition in solar-driven hydrogen permeation membrane reactor. *International Journal of Hydrogen Energy*. 2019;**44**(49): 26874-26887. DOI: 10.1016/j.ijhydene.2019.08.175

[69] Zhang L, Xu N, Li X, Wang S, Huang K, Harris WH, et al. High CO<sub>2</sub> permeation flux enabled by highly interconnected three-dimensional ionic channels in selective CO<sub>2</sub> separation membranes. *Energy & Environmental Science*. 2012;**5**(8):8310-8317. DOI: 10.1039/C2EE22045H

[70] Ceron MR, Lai LS, Amiri A, Monte M, Katta S, Kelly JC, et al. Surpassing the conventional limitations of CO<sub>2</sub> separation membranes with hydroxide/ceramic dual-phase membranes. *Journal of Membrane Science*. 2018;**567**:191-198. DOI: 10.1016/j.memsci.2018.09.028

[71] Wang H, Hao Y. Thermodynamic study of solar thermochemical methane steam reforming with alternating H<sub>2</sub> and CO<sub>2</sub> permeation membranes reactors. *Energy Procedia*. 2017;**105**: 1980-1985. DOI: 10.1016/j.egypro.2017.03.570